Carbohydrate Polymers 83 (2011) 727–736

Contents lists available at ScienceDirect

Carbohydrate Polymers

journal homepage: www.elsevier.com/locate/carbpol

Effect of processing history on the physicochemical and structural characteristics of starch–fatty acid extrudates plasticized with glycerol

S.N. Raphaelides*, G. Dimitreli, S. Exarhopoulos, G. Kokonidis, E. Tzani

Food Process Engineering Laboratory, Department of Food Technology, ATEI of Thessaloniki, P.O. Box 141, Thessaloniki GR-57400, Greece

ARTICLE INFO

Article history:
Received 16 April 2010
Received in revised form 30 July 2010
Accepted 18 August 2010
Available online 24 August 2010

Keywords:
Extrusion of thermoplastic starch
Starch–fatty acid–glycerol interactions

ABSTRACT

Normal maize starch was extruded in the presence of glycerol with and without the addition of fatty acid potassium salts in a twin-screw cooker extruder equipped with a slit die rheometer. The processing conditions employed were: heating at either 100 or 120 or 140 or 160 °C in all heated sections of the extruder and rotational screw speeds either 20 or 91 or 161 or 227 rpm. The in line melt viscosity measurements showed that the flow behaviour of the starch–glycerol system was significantly influenced by the addition of either myristic or palmitic acids. That is, the viscosity of the starch–fatty acid–glycerol systems was higher than that of the starch–glycerol systems regardless of the extrusion temperature employed whereas the flow behaviour index of the starch–fatty acid–glycerol systems was lower than that of the starch–glycerol systems. The examination of physicochemical properties of the extrudates such as bulk density, water solubility, expansion ratio and water adsorptivity indicated that the addition of fatty acids affected the functionality of starch–glycerol systems. Rheological studies revealed that the addition of fatty acids to starch–glycerol systems significantly affected their mechanical properties rendering them more flexible and less glassy than their counterparts which did not contain fatty acids. Structural studies indicated that the type of crystallites of starch–glycerol extrudates was different from that of starch–glycerol–fatty acid ones. The results led to the assumption of a possible interaction taken place between glycerol molecules and amylose–fatty acid complexes during extrusion cooking.

1. Introduction

Starch is considered as an attractive cheap source to be potentially utilized as a biodegradable material suitable to replace, at least to some extent, synthetic polymers mainly for environmental reasons. Starch is found in nature in the form of granules comprised of a biopolymer mixture of an essentially linear homopolymer of (1 → 4)-linked α-D-glucopyranose named amylose and its highly (1 → 6)-branched α-D-glucopyranose named amylopectin. The granules are water insoluble at ambient temperature while when they are heated in excess of water at temperatures around 70 °C, they undergo the so-called gelatinization process, i.e. they swell by absorbing water, the amylose solubilizes out of the granules and eventually the swollen granules mostly contained amylopectin become disrupted and the granular structure is lost (Cooke & Gidley, 1992; Parker & Ring, 2001). Upon cooling to ambient temperature, the starch components rapidly undergo the so-called retrogradation process, i.e. they crystallize out of the water. Besides, amylose is unique among the biopolymers having the ability to interact with polar and non-polar compounds such as fatty acids, fatty alcohols, monoglycerides and others, to form helical inclusion complexes.

Due to these properties, starch although it can be processed in the way the synthetic polymers are processed nevertheless it is difficult to handle and even to modify in order the products obtained to meet the requirements usually demanded for synthetic plastics in various industrial applications.

Among the various processes employed to convert native starch into a biodegradable material, extrusion cooking is the most prominent one. During extrusion of starch, the combination of shear, temperature and plasticizers makes possible the production of a molten thermoplastic material by disruption of the native crystalline granular structure and plasticization. This thermoplastic starch is rather unsuitable to use in packaging applications due to major drawbacks such as the changes occurring in its mechanical properties with time due to crystallization on aging, which makes it extremely rigid and easy to fracture and its tendency to absorb water.

When starch is extruded in the presence of lipids then the solubility of starch extrudates in water gets reduced (Bhatnagar & Hanna, 1994; Colonna & Mercier, 1983; Mercier, Charbonniere, Grebaut, & de la Gueriviere, 1980; Meuser, van Lengerich, & Stender, 1985b; Raphaelides, Arsenoudi, Exarhopoulos, & Xu, 2010; Stäger, 1988). Concerning, the crystallinity exhibited by these extrudates,

---

* Corresponding author. Tel.: +30 2310 791371; fax: +30 2310 791360.
E-mail address: rafael@food.teithe.gr (S.N. Raphaelides).

0144-8617/$ – see front matter © 2010 Elsevier Ltd. All rights reserved.
doi:10.1016/j.carbpol.2010.08.041

this is rather due to amylose–lipid complex formation than due to starch retrogradation and for this reason the crystal formation is much more rapid and increased than the crystal formation exhibited by starch extrudates contained no lipids (Raphaelides et al., 2010). Thus, starch–lipid interactions during extrusion cooking could be a method of producing biodegradable materials with tailor made properties. However, this is not so since starch–lipid extrudates are extremely glassy due to the removal of water from their structure thus to become flexible it might be necessary to add a natural plasticizer such as glycerol to reduce the glass transition temperature.

To the best of our knowledge, the processing behaviour and the functionality of starch–fatty acid extrudates plasticized with glycerol has not been investigated so far. The aim of this work is to explore the production of starch–lipid extrudates in the presence of glycerol under various processing conditions and to assess their structural and functional characteristics in the hope that some of these extrudates could exhibit technological characteristics suitable for industrial applications.

2. Materials and methods

2.1. Materials

Commercial maize starch was purchased from Nestlė Hellas, Greece. The starch characteristics were: moisture content 12.0%[1], apparent amylose 21.5 ± 0.6%[2], total amylose 26.0 ± 0.3%[2], onset gelatinization temperature 67.5 ± 0.6 °C[3], peak gelatinization temperature 72.0 ± 0.5 °C[3].

Myristic acid (purity > 98.5%) was purchased from Fluka, palmitic acid (purity > 95%) was purchased from Sigma Chemical Co and glycerol (purity > 90%) was obtained from Carlo Erba. Salts used to prepare solutions of known water activity were: LiCl (>99%), $MgCl_2{\cdot}6H_2O$ (>99%), K_2CO_3 (>99%), $Mg(NO_3)_2$ (>99%) purchased from Fluka, NaCl (>99%) obtained from Merck and KNO_3 (>99%) from Riedel-de Haën. All other reagents used were of analytical grade.

2.2. Extrusion conditions

Extrusion cooking was performed in a pilot scale co-rotating intermeshing twin-screw extruder, Clextral model BC45, France. The barrel was 550 mm in length and 110 mm in diameter, with two heating zones heated with induction heaters and cooled with circulating tap water. At the barrel's end, a slit die rheometer was attached through a transition attachment having the shape of a truncated conical neck to provide smooth hydrodynamic transition from the extruder to the die entrance. Both the neck and the slit die rheometer were custom made in a local workshop. The length of the neck was 120 mm and that of the rheometer was 250 mm. The rectangular cross-section of the slit die was 20 mm wide and the height was 1.5 mm. Both the neck and the rheometer were equipped with centrally placed type K thermocouples. The rheometer was also equipped with high temperature Gefran, Italy (SP830 M series), pressure transducers, flush mounted along the length of the die with pressure range 0–20 and 0–10 MPa, respectively. The rheometer was heated by means of electric cartridge heaters which covered all the available external surface of the rheometer and cooled by means of circulating tap water.

All process variables, i.e., temperatures measured at every zone of the barrel, the neck and the rheometer, pressures from the pressure transducers, rotational speed of the screws, current and power input from the extruder's motor were continuously logged, in real time mode, on a PC through a data acquisition card constructed, and programmed at our electronics workshop. The solid feed was transferred from a hopper, mounted on the extruder, through a controlled speed screw feeder to an opening located in the entrance of the barrel whereas the liquid feed was transported to the opening of the barrel's entrance by means of a metering diaphragm pump from a temperature controlled jacketed vessel equipped with a variable speed stirrer.

2.3. Experimental design

In all experimental runs the extruder was operated in the starve fed mode. The degree of fill, expressed as *g* of feed material/rpm of screw speed (van Lengerich, 1989) was kept constant at 3.0. As for the solid/liquid ratio of the feed material, it was 2:1 in all experimental runs.

Three series of samples were obtained from the respective experimental runs. That is

1st Run: the feed material was a mixture of starch, water and glycerol (control).
2nd Run: the feed material was a mixture of starch, glycerol and aqueous solution of potassium myristate salt.
3rd Run: the feed material was a mixture of starch, glycerol and aqueous solution of potassium palmitate salt.

The experimental scheme applied in all three runs was the following

Sample	Throughput rate (solid + liquid) (kg/h)	Extrusion processing temperature (°C)	Screw speed (rpm)
1	3.60	100	20
2	16.38	100	91
3	29.01	100	161
4	40.81	100	227
5	3.60	120	20
6	16.38	120	91
7	29.01	120	161
8	40.81	120	227
9	3.60	140	20
10	16.38	140	91
11	29.01	140	161
12	40.81	140	227
13	16.38	160	91
14	29.01	160	161
15	40.81	160	227

In all heated sections of the extruder system and for each sample, the selected temperatures were the same. The fatty acid concentration corresponded to 1.76% of the starch solids, whereas the glycerol concentration corresponded to 13.3% of the total feed weight. The feed solution (either with or without fatty acid) was kept, under continuous stirring, throughout the experiments at 60 °C to avoid micelle formation in the feed vessel.

2.4. In line viscosity determination of the extrudate melts

Melt viscosity determination was based on the process parameters recorded on line through out the course of the extrusion processing runs. The rheological equations used were obtained from Han's (1976) analysis.

That is, the shear stress was calculated from the equation

$$\tau = \frac{\Delta P * H}{2 * L}\,(\mathrm{Pa}) \qquad (1)$$

---

[1] Gravimetrically determined by heating the samples at 130 °C for 1 h.

[2] Determined using the method of Morrison and Laignelet (1983).

[3] Onset and peak gelatinization temperatures measured with a Perkin-Elmer DSC-6 differential scanning calorimeter.

where ΔP is the pressure drop between the pressure sensors, H is the height of the slit (mm), and L is the distance between the pressure sensors (mm).

The wall apparent shear rate was calculated from the equation

$$\dot{\gamma}_{\text{app}} = \frac{3Q}{2B * h^2}\,(\text{s}^{-1}) \tag{2}$$

where Q is the volumetric flow rate in the slit (mm^3/s), B is the width of the slit (mm), and h is the 1/2 of the slit height (mm).

The corrected shear rate was calculated according to the method of Rabinowitsch (Han, 1976) as follows

$$\dot{\gamma}_{\text{corr}} = \left(2n + \frac{1}{3n}\right) * \left(\frac{3Q}{2B * h^2}\right)(\text{s}^{-1}) \tag{3}$$

where n is the flow behaviour index $(\partial \ln \tau)/(\partial \ln \dot{\gamma}_{\text{app}})$, the rest of the symbols are the same as in Eq. (2).

The apparent viscosity was calculated from the power law equation

$$\eta = m * \dot{\gamma}_{\text{corr}}^{n-1} \quad (\text{Pa s}) \tag{4}$$

where m is the consistency index.

All samples after preparation and prior to their examination were stored for eight days at room temperature so that their moisture content to be equilibrated. Preliminary studies showed that this period of time was quite sufficient for sample stabilization as far as their functional characteristics are concerned.

2.5. *Specific mechanical energy (SME)*

The extruder was driven by a DC motor powered from 3-phase mains through controlled rectifier of thyristor for speed regulation. The SME provided by the motor of the extruder during the extrusion cooking process was calculated using the following equation:

$$\text{SME} = \text{ME} - \text{TE} = \frac{(V * I) - (I^2 * R)}{m}\,(\text{Wh} * \text{kg}^{-1}) \tag{5}$$

where ME is the mechanical energy provided by the motor to the extruder, TE is the thermal loss due to electrical resistance in the motor (Joule effect), V is the voltage applied to the armature of the motor (V), I is the current (A), m is the feed rate supplied to the extruder (kg/h).

Since, $(V–IR)$ is proportional to the screw speed, it can be measured from the speed setting signal. The current signal was taken from the meter. Both signals were at mains potential, therefore were fed to the computer connected to the extruder, through optocoupler for insulation and V–F, F–V converter signal accuracy.

2.6. *Moisture content*

It was gravimetrically determined by heating the samples at 130 °C for 90 min.

2.7. *Bulk density*

It was determined using a volume displacement technique as follows: In a preweighed graduated cylinder, capacity 250 mL, 140 mL of n-hexane were added and the cylinder was reweighed. An approximately 12 cm in length of weighed extrudate sample was fully submerged inside the cylinder and by means of a positive displacement mechanical pipette the displaced volume of the n-hexane was carefully transferred to a dry preweighed beaker and the beaker was again weighed. Since the density of n-hexane is known to be 655 kg/m^3, the volume of the displaced n-hexane can be easily and accurately measured. The volume of the displaced n-hexane is equal to the volume of the sample, thus the bulk density of the sample can be calculated by dividing the mass of the sample by its volume. The measurements were replicated three times.

2.8. *Expansion ratio*

The determination of the cross-sectional area of the samples was quite difficult due to irregularities most of them exhibited on their surface. Hence, it was decided to use the following technique: The length of the samples was accurately measured using a digital vernier caliper. From bulk density determination the volume of the sample was known. Thus, dividing the volume by the length, the average cross-sectional area of the sample was obtained. The expansion ratio was calculated by dividing the cross-sectional area of the samples by the cross-sectional area of the slit die.

2.9. *Water solubility index (WSI)*

WSI, defined as the water soluble fraction of the extrudate expressed as percentage of dry sample and being a measure of the dispersibility of the material was measured by the method of Anderson, Conway, Pfeifer, and Griffin (1969).

2.10. *Adsorption isotherms*

Extrudate samples were dried in a vacuum oven at 50 °C for at least 24 h, till constant weight. Quantities (~0.5 g) of the dried samples, contained in preweighed polypropylene dishes, were weighed in an analytical balance and placed over saturated (at 40 °C) salt solutions of known relative humidity values in hermetically sealed glass containers (capacity 800 mL). Then, the containers were stored in a thermostatically controlled chamber at 30 °C. The dishes were weighed, at regular time intervals, till constant weight. It was found that equilibrium was achieved after a week. The adsorption experiments were replicated three times. The adsorption isotherms were drawn using as coordinates the parameters, percentage relative humidity and water content, i.e. the weight difference of the sample at the beginning of the storage period at a certain relative humidity environment and after the equilibrium in this environment was achieved, over the initial weight of the dried sample.

2.11. *Limiting viscosity number (intrinsic viscosity)*

Finely cut (thickness 25 μm), in a microtome, pieces of extrudate samples were dissolved in aqueous solution of 1N KOH, at 60 °C under periodic swirl mixing. The solutions were diluted with distilled water to 0.1N and then they were filtered through Gooch fritted glass filter no. 2 to remove minute quantities of undissolved particulate material. The specific viscosity (η_{sp}) of the solutions was measured using an Ubbelohde suspended level type viscometer which was kept in a water bath at 20 ± 0.1 °C. The flow time of the solvent (0.1N KOH) was 130 s. The initial starch concentration of the filtered solutions was around 4 mg/mL, accurately determined using an enzymic method (Karkalas, 1985). The intrinsic viscosity was determined from the gradient by using linear regression on the viscosity number (η_{sp}/c)–concentration (c) data, according to the method described by Greenwood (1964).

2.12. *Modulus of elasticity and rheological glass transition temperature*

Extrudate samples were cut into strips of dimensions 36 mm × 10 mm × 3 mm and were measured in a DMA rheometer Bohlin CVOR 150 (Malvern, UK), operated in the oscillatory mode under constant frequency 0.1 Hz, constant stress 150 Pa and programmed heating rate of 5°C/min. The strain in all samples examined ranged from 10×10^{-7} to 10×10^{-5} which was well within the linear viscoelastic region. The parameters measured were the storage modulus G' and $\tan\delta$ in relation to the temperature of heating. Glass transition temperature was determined from the position of $\tan\delta$ peak observed for most extrudates.

2.13. Three-point bending test

Extrudate samples cut into strips were measured in an Instron UTM, table model 1140 (Instron, UK), equipped with a 50 kg maximum load force cell and operated in compression mode through a custom made software. A set of three-point bending accessory was attached to the measuring unit of the instrument. The sample was held on two stationary bending supports 85 mm apart while being displaced at a central axis by the bending probe attached to the moving crosshead traveling at a speed of 0.083 mm/s. The final displacement was 10% of the sample thickness. The test was employed to determine Young's modulus of elasticity (E) using the following equation (Steffe, 1996):

$$E = \frac{Fa^3}{4d * b * h^3} \tag{6}$$

where a is the length between the stationary beams(supports), b is the width of the sample, h is the thickness of the sample, and d is the displacement.

Each sample was measured in triplicate and averaged.

2.14. X-ray diffraction

Extrudate samples were immersed in liquid nitrogen and immediately were pulverized by means of a pestle and a mortar. The powder obtained was passed through a sieve with an aperture of 800 μm. X-Ray powder diffraction measurements were carried out using a PANalytical X'Pert Pro diffractometer (Panalytical, Netherlands) with a Cu $\text{K}\alpha_1$ radiation (λ = 1.5405980 Å). The diffractometer was operated in reflection mode at 45 kV and 40 mA. A divergence slit of 1°, an antiscatter slit of 2° and a receiving slit of 0.4 mm were used. Measurements were taken between 6° and 35° (2θ) with a step size of 0.04° and a scan speed of 0.008°/s.

For the determination of the relative crystallinity the data were normalized from 9° to 30° (2θ) and the background was determined using the X'Pert HighScore PANalytical software. The crystallinity index (X_c) was calculated according to the following equation (Stribeck, 2007):

$$X_c = \frac{I_{cr}}{I_{am} + I_{cr}} \tag{7}$$

where I_{cr} is the integrated area between the crystalline reflections and the amorphous halo and I_{am} the integrated area between the amorphous halo and the baseline.

Crystallite size was determined according to Scherrer's formula (Brundle, Evans, & Wilson, 1992):

$$L \approx \frac{\lambda}{\text{FWHM} \times \cos\theta} \tag{8}$$

where L is the crystallite size in Å, λ is the wavelength and FWHM is the Full Width at Half-Maximum.

2.15. Scanning electron microscopy

Extrudate samples were mounted on aluminum stubs with sticky double-side carbon tape. No special treatment applied to the specimens and no coating was needed. Examination was performed by a Carl Zeiss EVO 50 VP scanning electron microscope (Carl Zeiss SMT, Ltd., UK) at 5 kV accelerating voltage, under variable pressure mode, suitable for non-conductive specimens, at pressure of 30 Pa. A Variable Pressure Secondary Electron (VPSE) detector was used.

3. Results and discussion

In all extrusion experiments the quantity of fatty acids used was calculated to be 5% in excess to that needed to fully saturate the available amylose helices (Karkalas & Raphaelides, 1986), provided that all molecules of apparent amylose would be in position to interact freely with the fatty acid molecules. The fatty acids were added to starch as soap aqueous solution in order their molecules to be in their most active form, i.e. as monomers. These precautions were taken since the available water in the starch system was limited and it was imperative to secure the best possible dispersibility of the fatty acid anions so to achieve the maximum degree of interaction between the starch molecules and the fatty acid anions.

3.1. Flow behaviour of starch–glycerol–fatty acid extrudate melts

Fig. 1 shows the flow curves obtained for the three systems examined, i.e. starch–water–glycerol (control), starch–myristate soap solution–glycerol and starch–palmitate soap solution–glycerol at different slit die temperatures (100–120–140–160 °C). It can be seen that the samples contained fatty acid exhibited higher viscosities than the control samples, regardless the extrusion temperature employed. This has been attributed (Raphaelides et al., 2010) to the fatty acid interaction with amylose and the formation of helical complexes. It is known (Banks & Greenwood, 1971; Carlson, Larsson, Dinh-Nguyen, & Krog, 1979; Godet, Tran, Delage, & Buleon, 1993; Snape, Morrison, Maroto-Valer, Karkalas, & Pethrick, 1998), that the helical cavity is hydrophobic whereas at the outer surface of the helix, active amylosic hydroxyl and fatty acid carboxyl groups are exposed enabling adjacent amylose helices to interact, possibly through hydrogen bonding, with each other and to form supermolecular structures, i.e. a kind of quaternary structure. Thus, the hydrodynamic volume of the molecular systems considerable increases with the result, the increase in viscosity of the starch–fatty systems. The higher viscosity exhibited by the starch–palmitate system in comparison to that of the starch–myristate system could be attributed to the stiffer nature of amylose–palmitate helices in comparison to amylose–myristate helices. It is known (Karkalas & Raphaelides, 1986) that saturated, with fatty acid molecules, amylose helices accommodate in their cavity fewer palmitate ions than myristate ones per unit length because palmitate molecules are longer than the myristates. Thus, amylose–palmitate helices have fewer kinks than amylose–myristate ones and their conformation becomes stiffer whereas amylose–myristate helices are more flexible. Hence, the hydrodynamic volume of the supermolecular structure of the starch–palmitate system retained its size during flow even at high shear rates to a greater degree, than that of the starch–myristate system. It has to be noted that the pseudoplasticity (expressed by the flow behaviour index) of starch–fatty acid extrudates was much higher (low index values) than that of the control especially at the higher extrusion temperatures employed. This should be attributed not only to the dissociation of the formed supermolecular structure, which was previously mentioned, but also due to the orderly arrangement of the elongated amylose helices at high shear rates causing the significant reduction in viscosity.

Besides, the samples contained fatty acids displayed, paradoxically, lower viscosities at 100 °C at rather low shear rates than those exhibited at 120 °C at the same low shear rates (Fig. 1a and b). This can be attributed to incomplete gelatinization of starch granules occurred in the presence of fatty acids at 100 °C, which helped a number of starch granules to retain their shape albeit swollen as shown by SEM micrographs (Fig. 6) Thus, the samples

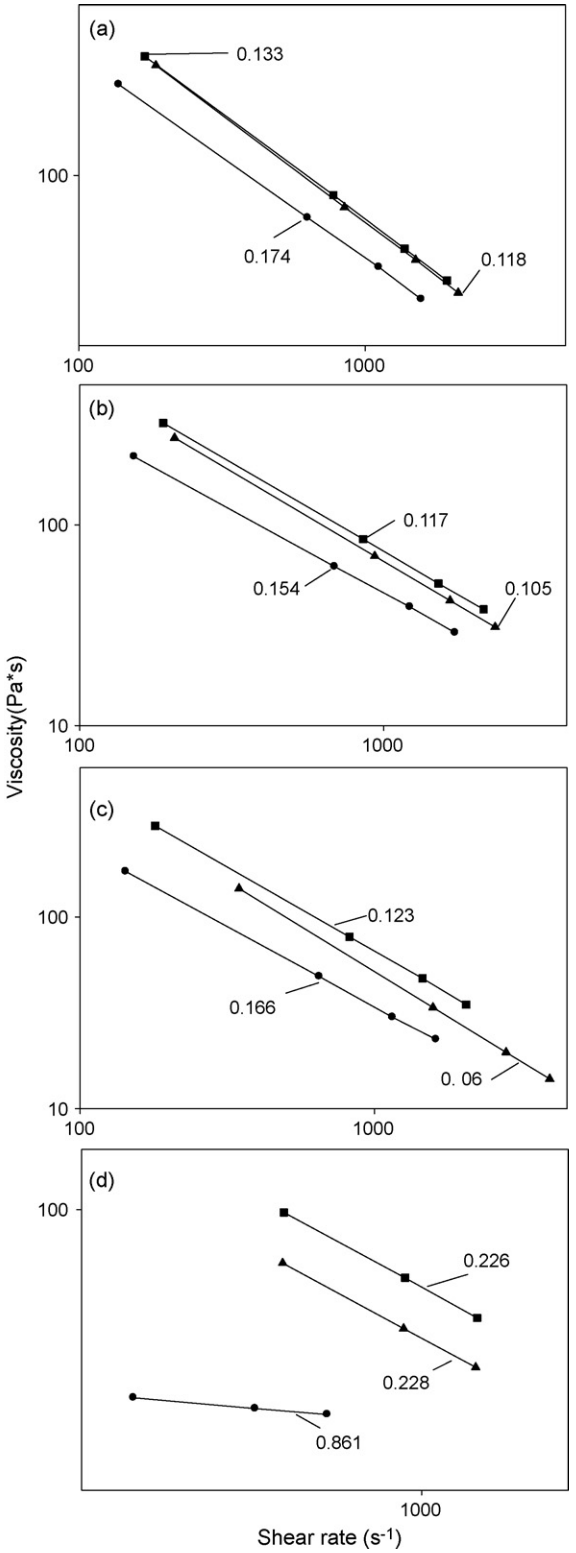

Fig. 1. Effect of heating temperature on the flow behaviour of starch–fatty acid–glycerol extrudate melts. ●, Control sample (no fatty acid added); ▲, sample with added myristic acid; ■, sample with added palmitic acid. (a–d) Denote heating temperatures of 100, 120, 140 and 160 °C, respectively. Numbers attached to the flow curves denote the flow behaviour index of the individual curve.

exhibited lower viscosities at 100 °C than at 120 °C whereas it should have been the opposite. Since, all samples (including the control ones) contain the same amount of glycerol this incomplete gelatinization, occurred only in the fatty acid containing samples, should not be attributed, at least solely, to the lubricating effect of glycerol but mostly to the effect of the fatty acid present. That is, the starch–fatty acid interactions taken place during gelatinization, increased the elasticity of the granules to some extent, however sufficient enough to withstand the shearing forces applied to them during extrusion. It has been demonstrated (Raphaelides, 1992) that the addition of fatty acids to starch solutions, in quantities sufficient to saturate the available amylose helices, increased the elasticity exhibited by starch systems in 0.01N KOH aqueous solution, expressed in the form of normal force measurements during steady shear experiments.

3.2. *Specific mechanical energy (SME)*

The amount of SME input during the extrusion process is considered as an indication of the severity of the structural modifications the feed material undergoes during extrusion. Fig. 2a shows the SME input at the specified barrel temperatures during extrusion of maize starch–water–glycerol–fatty acid systems in

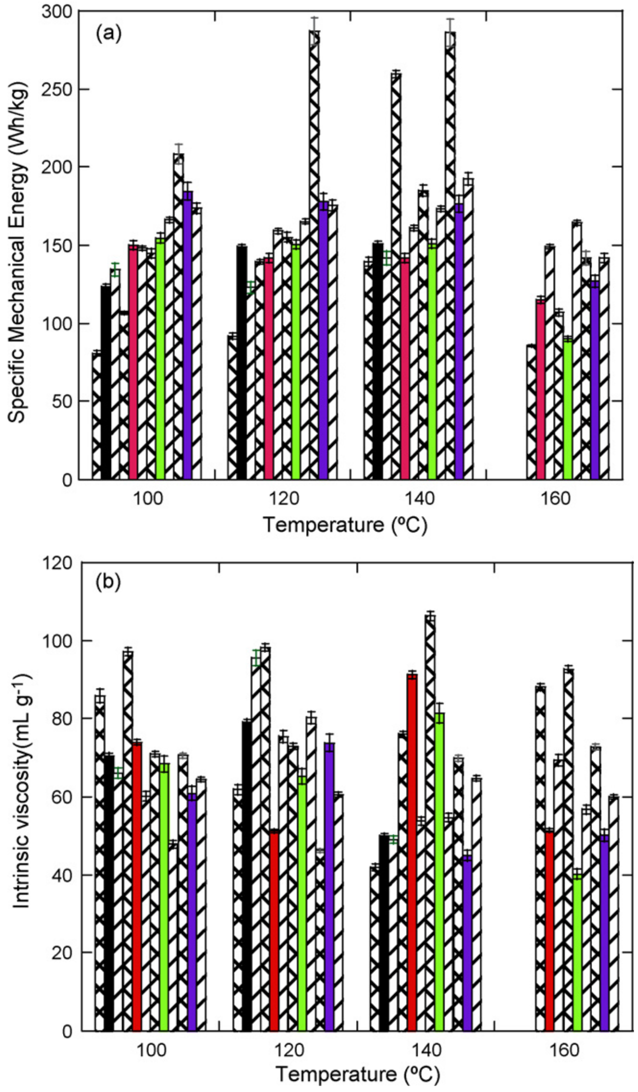

Fig. 2. (a) Effect of screw speed and barrel temperature on the specific mechanical energy of starch–fatty acid–glycerol extrudates. (b) Effect of screw speed and barrel temperature on the intrinsic viscosity of starch–fatty acid–glycerol extrudates Crossed line columns: control samples (no fatty acid added); filled columns: samples with added myristic acid; inclined line columns: sample with added palmitic acid. Column colours denote screw speeds: black, 20 rpm; red, 91 rpm; green, 161 rpm; blue, 227 rpm. (For interpretation of the references to color in this figure legend, the reader is referred to the web version of the article.)

relation to screw speed. It can be seen that for almost all samples, SME input was screw speed dependent. That is, the higher the screw speed employed the higher the SME attained. Moreover, the pattern of SME increase remained more or less the same for all extrusion temperatures, with the samples containing fatty acid to require more energy during their extrusion than their control counterparts, with the notable exception of control samples extruded at the highest screw speed employed (227 rpm) at 100, 120 or 140 °C extrusion temperature. The higher SME values observed for the fatty acid containing samples could be attributed to significant conformational changes occurred to them as previously mentioned which caused the increase in energy consumption during their flow through the extruder's barrel and the slit rheometer. On the other hand the remarkable increase of SME consumption for the control samples extruded at high screw speed is puzzling and difficult to explain. As for the fairly lower SME values observed for the samples extruded at 160 °C in comparison to the SME values attained for the analogous samples at lower temperatures it should be attributed to the significantly lower viscosities exhibited by all samples at this temperature.

3.3. *Intrinsic viscosity*

Intrinsic viscosity ($[\eta]$) as a measure of starch degradation (depolymerization) during extrusion, has been used by a number of workers (Colonna & Mercier, 1983; Colonna, Doublier, Melcion, de Monredon, & Mercier, 1984; Davidson, Paton, Diosady, & Larocque, 1984; Launay & Koné, 1984). Moreover, it has been reported (Della Valle, Kozlowski, Colonna, & Tayeb, 1989; Parker, Ollett, & Smith, 1990) that SME is inversely related to intrinsic viscosity. Fig. 2b shows the $[\eta]$ values exhibited by starch–glycerol–fatty acid extrudates as a function of barrel temperature and screw speed. The $[\eta]$ of native maize starch determined under the same experimental conditions employed for the extrudate samples, was found to be 144.50 mL/g. It can be seen, that all extrudate samples regardless of whether they contained fatty acid or not showed lower $[\eta]$ values than that of the native starch. This is an indication that all extrudates have undergone a certain degree of starch modification, possibly degradation. As a matter of fact, most of the control samples attained higher intrinsic viscosity values than their fatty acid containing counterparts. Moreover, there seems to be a relation between the SME values and the respective intrinsic values for the majority of control samples which support the findings of Della Valle et al. (1989) that the intrinsic viscosity is inversely proportional to SME.

However, in the case of the fatty acid containing samples there is no a clear indication that this relation exists and this is something to be expected. It has been demonstrated (Karkalas & Raphaelides, 1986) that the intrinsic viscosity of amylose molecules was dramatically reduced in the presence of added fatty acids, due to amylose–fatty acid interactions which caused changes in amylose's conformation from random coil to helix resulting in the significant reduction to its hydrodynamic volume. Thus, the intrinsic viscosity can be used as a tool for assessing starch degradation in the case of uncomplexed starch systems whereas in the case of complexed starch systems it should be regarded with caution. Nevertheless, the findings indicate that the starch–glycerol–fatty acid samples do undergo a kind of structural modification during extrusion cooking. Similar findings were reported for non-containing glycerol starch–fatty acid extrudates (Raphaelides et al., 2010).

3.4. *Functional properties of starch–glycerol–fatty acid extrudates*

Table 1 shows the moisture contents of starch–glycerol–fatty acid extrudates at various screw speeds and barrel temperatures. It can be seen that the moisture content of control samples, in general, is higher than that of the starch–fatty acid samples. This is possibly due to the formation of the crystalline type II polymorph V-structure of the amylose–fatty acid complexes which is known (Biliaderis & Seneviratne, 1990) to be very compact, thus fewer water molecules remained trapped among the amylose helices. The lower moisture content of the samples extruded at higher temperatures should be attributed to water evaporation occurred at the exit of the die due to the high temperature difference between the extruder's die interior and the atmospheric environment. It has to be noted that samples contained myristic acid had lower moisture content than the other samples possibly due to more efficient complexation of amylose–myristate ions (Meuser, van Lengerich, & Stender, 1985a) hence the formation of a more compact structure in comparison to the other samples.

Concerning bulk density of the extrudates it can be seen (Table 1) that in general, the bulk density exhibited by all samples was rather screw speed than barrel temperature dependent. That is, the higher the screw speed the lower the bulk density attained by the extrudates. Besides, this effect is more pronounced at higher extrusion temperatures. This behaviour can be attributed to the degradation of starch structure occurred at high screw speeds and at high extrusion temperatures which caused the samples to acquire a more open structure. As a matter of fact most of the samples with low bulk density values showed higher expansion ratio values than the other samples (Table 1) and this supports the assumption of open structure.

As for the water solubility index (WSI), it can be seen (Table 1) that most of the samples containing fatty acids showed lower WSI values than the control samples and this should be due to the hydrophobic behaviour of the amylose–fatty acid complexes they contained as it has been already stated in the introduction.

3.5. *Adsorption isotherms*

Adsorption isotherm experiments indicated that the behaviour of all extrudate samples regardless of whether they contained lipids or not, was rather similar. Fig. 3 shows typical examples of isotherms of control extrudates and extrudates containing palmitic acid as a function of heating temperature (Fig. 3a) and control extrudates and extrudates containing myristic acid as a function of the screw speed (Fig. 3b). The shape of all curves is rather peculiar and especially for the samples containing fatty acids, it appears to be bimodal, i.e. for low relative humidity values (<40%) limited moisture adsorption was observed which was gradually reduced up to approximately 40% relative humidity whereas at higher relative humidity values the adsorption capacity of the extrudates was progressing as the relative humidity was rising. Similar shape of adsorption isotherms was also observed in the case of heated at 100 °C starch–sorbitol systems with either added fatty acids or without (Mantzari, Raphaelides, & Exarhopoulos, 2010). Attempts were made to find out whether sorption isotherm models such as GAB, BET or others could be used to describe the isotherms. However, it was found that no model satisfactorily fits for a fairly wide range of relative humidities. Especially, one of the GAB parameters was found to have negative values for all isotherms examined and thus rejected because of physical impossibility. Bizot (1983) emphasized that GAB model does not fit for starch when it becomes more crystalline at water activities from 0.6 to 0.7.

3.6. *Three-point bending*

Fig. 4 shows the rigidity exhibited by starch–glycerol extrudate samples with added myristic acid or without (control) expressed as Young's modulus values. It can be seen that concerning the control samples the rigidity shown is both barrel temperature as well as

Table 1
Effect of screw speed and barrel temperature on the functional properties of maize starch-fatty acid-glycerol extrudates.[a]

Sample	Screw speed (rpm)	Barrel temperature (°C)	Moisture content (%)	Bulk density (kg/m^3)	Expansion ratio	Water solubility index (%)	Glass transition temperature (°C)
Control	20	100	16.1 ± 0.5	1282 ± 5	1.64 ± 0.02	17.7 ± 0.2	59 ± 2.0
Starch + myristate			16.0 ± 0.2	1190 ± 2	1.20 ± 0.05	13.6 ± 0.5	62.2 ± 4.0
Starch + palmitate			15.1 ± 0.5	1387 ± 4	1.29 ± 0.07	14.4 ± 0.1	Not observed
Control		120	13.3 ± 0.2	1437 ± 2	1.86 ± 0.05	12.4 ± 0.5	82.2 ± 0.5
Starch + myristate			11.8 ± 0.5	1378 ± 5	1.13 ± 0.01	13.7 ± 0.2	Not observed
Starch + palmitate			14.4 ± 0.5	1328 ± 6	1.17 ± 0.02	12.1 ± 0.3	65.0 ± 3.0
Control		140	11.3 ± 0.5	1410 ± 15	2.16 ± 0.01	11.4 ± 1.5	80.1 ± 2.0
Starch + myristate			13.6 ± 0.1	1206 ± 5	1.28 ± 0.05	12.6 ± 0.5	37.5 ± 1.0
Starch + palmitate			11.9 ± 0.2	1316 ± 8	1.30 ± 0.02	14.6 ± 0.5	77 ± 0.8
Control	91	100	17.1 ± 0.2	1276 ± 5	2.49 ± 0.07	16.4 ± 0.8	60.7 ± 1.0
Starch + myristate			13.0 ± 0.5	1148 ± 2	1.42 ± 0.05	12.4 ± 0.3	53.2 ± 1.0
Starch + palmitate			14.7 ± 0.4	1119 ± 4	1.37 ± 0.02	16.1 ± 0.3	52.5 ± 1.5
Control		120	15.4 ± 1.0	1401 ± 3	2.54 ± 0.02	13.3 ± 0.5	73 ± 2.0
Starch + myristate			14.9 ± 0.3	1286 ± 4	1.43 ± 0.02	12.8 ± 0.2	36.0 ± 1.0
Starch + palmitate			12.3 ± 0.4	1222 ± 7	1.625 ± 0.01	12.7 ± 0.2	Not observed
Control		140	13.1 ± 0.4	773 ± 2.0	4.89 ± 0.02	11.2 ± 0.2	75 ± 2.5
Starch + myristate			14.2 ± 1.0	1253 ± 5.0	1.80 ± 0.02	8.8 ± 0.4	36.2 ± 1.0
Starch + palmitate			10.7 ± 0.8	1206 ± 5.0	1.86 ± 0.05	9.8 ± 0.4	52.6 ± 1.5
Control		160	14.0 ± 0.5	914 ± 5.0	1.44 ± 0.01	17.4 ± 2.0	75.0 ± 1.0
Starch + myristate			12.6 ± 0.8	1339 ± 3.0	2.11 ± 0.03	7.7 ± 0.5	34.3 ± 2.0
Starch + palmitate			10.9 ± 0.7	1353 ± 6.0	1.97 ± 0.07	11.3 ± 0.4	Not observed
Control	161	100	17.7 ± 1.0	1029 ± 5	2.11 ± 0.03	11.1 ± 0.8	63 ± 3.0
Starch + myristate			14.9 ± 0.6	1083 ± 8	1.65 ± 0.01	7.4 ± 0.8	Not observed
Starch + palmitate			13.8 ± 0.2	1115 ± 3	1.80 ± 0.02	14.5 ± 1.0	48.2 ± 1.0
Control		120	16.7 ± 1.5	1261 ± 3	2.75 ± 0.1	14.8 ± 0.3	72.2 ± 1.0
Starch + myristate			16.8 ± 1.0	1335 ± 2	1.56 ± 0.07	11.1 ± 0.1	Not observed
Starch + palmitate			14.6 ± 0.8	1049 ± 6	1.83 ± 0.03	10.1 ± 0.2	52.0 ± 2.0
Control		140	15.1 ± 1.0	794 ± 4	7.22 ± 0.08	20.2 ± 1.0	73.8 ± 2.0
Starch + myristate			11.9 ± 0.1	1139 ± 3	2.21 ± 0.03	6.0 ± 0.05	29.0 ± 2.0
Starch + palmitate			11.5 ± 0.2	1098 ± 5	2.37 ± 0.07	11.1 ± 0.02	72.6 ± 1.5
Control		160	15.1 ± 0.4	1219 ± 7	2.93 ± 0.04	21.5 ± 1.00	76.4 ± 1.7
Starch + myristate			11.5 ± 0.3	1091 ± 5	1.57 ± 0.05	10.1 ± 0.03	29.8 ± 1.0
Starch + palmitate			10.5 ± 0.3	982 ± 2	3.06 ± 0.03	7.5 ± 0.01	73.7 ± 1.5
Control	227	100	16.0 ± 1.4	1161 ± .4	3.18 ± 0.41	13.0 ± 0.04	68 ± 3.0
Starch + myristate			12.2 ± 0.6	1088 ± 2	2.79 ± 0.02	8.3 ± 0.02	30 ± 1.0
Starch + palmitate			12.4 ± 1.1	884 ± 6	2.48 ± 0.03	8.0 ± 0.14	Not observed
Control		120	13.9 ± 0.4	789 ± 4	3.43 ± 0.04	15.8 ± 0.09	64.1 ± 3.0
Starch + myristate			13.2 ± 0.7	1051 ± 7	2.43 ± 0.01	5.7 ± 0.11	Not observed
Starch + palmitate			12.4 ± 0.3	1023 ± 5	2.34 ± 0.08	5.1 ± 0.21	46.9 ± 1.8
Control		140	10.3 ± 0.5	792 ± 8	4.41 ± 0.24	5.8 ± 1.4	81.7 ± 2.0
Starch + myristate			12.5 ± 0.8	984 ± 3	3.00 ± 0.11	5.2 ± 0.5	35.2 ± 3.0
Starch + palmitate			10.4 ± 0.1	1066 ± 6	3.27 ± 0.04	11.5 ± 0.1	Not observed
Control		160	15.3 ± 0.4	765 ± 2	3.90 ± 0.14	15.0 ± 0.4	77.8 ± 1.0
Starch + myristate			13.5 ± 0.7	1039 ± 4	3.11 ± 0.08	3.3 ± 0.2	Not observed
Starch + palmitate			9.7 ± 0.9	832 ± 7	3.57 ± 0.19	7.3 ± 0.3	35.4 ± 1.4

[a] All samples contained the same amount of glycerol.

screw speed dependent. That is, at 20 rpm screw speed the sample's stiffness increased with the temperature increase up to 140 °C whereas at higher screw speeds the rigidity was gradually reduced as the barrel temperature increased. As for the samples containing myristic acid the rigidity exhibited by all samples was much lower than that shown by their control counterparts. The results indicated that in the case of the control samples the presence of glycerol caused a much lower plasticization effect in comparison to that caused in the case of the starch–fatty acid systems. It should be mentioned that the glycerol content in all extrudate samples examined is estimated to be 18–20%, which is higher to that (12%) considered to cause antiplasticization effects to starch systems (Lourdin, Bizot, & Colonna, 1997). This increase of glycerol content from the initial 13.3% fed to the extruder to the 18–20% contained in the extrudate product is due to evaporation of part of the initial water content in the feeding zone occurred at the extruder's exit because of the high temperatures employed throughout the extruder's system. The higher flexibility shown by the myristic acid containing samples could be attributed to the more effective incorporation and possibly more uniform distribution of glycerol molecules to the starch matrix in these samples in comparison to the control samples. The amylose–fatty acid interactions taken place during extrusion cooking caused rapid formation of crystallites made of amylose–fatty acid helices with the result the structure of the starch matrix quickly is organized in a controlled and stable fashion. As it has been previously mentioned, during amylose–fatty acid complexation the formed helices bear on their surface active hydroxyl groups which it is possible to interact with glycerol molecules through hydrogen bonding enhancing the plasticization effect of glycerol, something which might be less

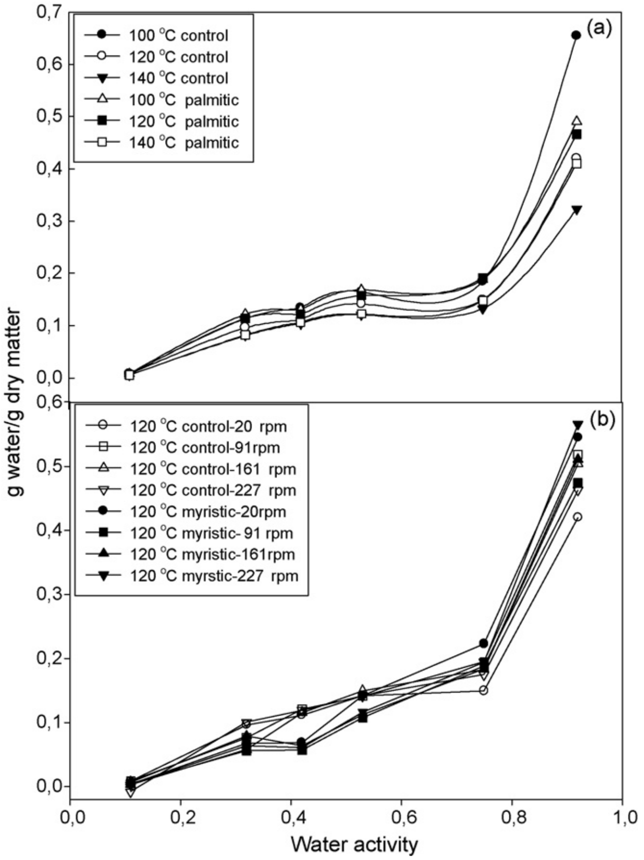

Fig. 3. Adsorption isotherms of starch–fatty acid–glycerol extrudates. (a) Control samples and samples with added palmitic acid extruded at barrel temperatures: 100–120–140–160 °C. Screw speed: 20 rpm. (b) Control samples and samples with added myristic acid extruded at barrel temperature 120 °C and screw speeds: 20–91–161–227 rpm.

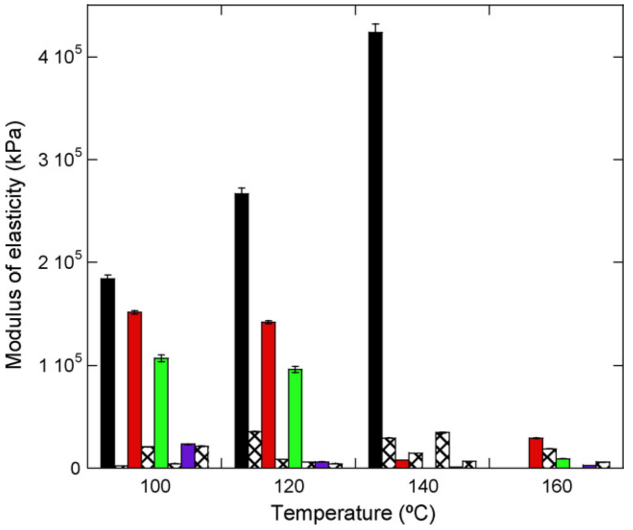

Fig. 4. Effect of screw speed and barrel temperature on the modulus of elasticity of starch–fatty acid–glycerol extrudates. Filled columns: control samples (no fatty acid added); crossed line columns: samples with added myristic acid. Column colours denote screw speeds: black, 20 rpm; red, 91 rpm; green, 161 rpm; blue, 227 rpm. (For interpretation of the references to color in this figure legend, the reader is referred to the web version of the article.)

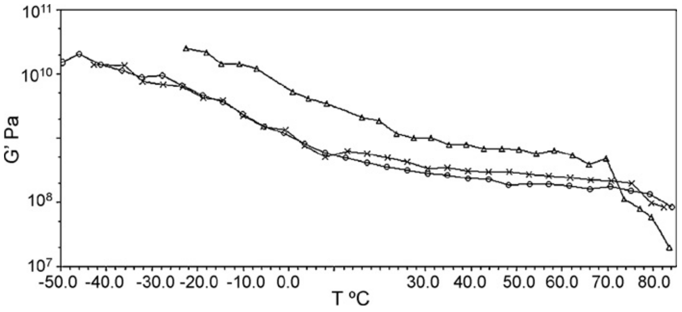

Fig. 5. Storage modulus (G') versus barrel temperature of starch–glycerol systems extruded with the addition of fatty acids or without (control). Symbols: △, control, *, myristic acid, ○, palmitic acid. Frequency of oscillation, 0.1 Hz; stress applied, 150 Pa; heating rate, 5 °C/min.

pronounced in the case of the control samples. In the control samples, most of the crystallites are formed after extrusion and during aging and mainly consist of retrograded amylose helices which might not have the ability to effectively interact with glycerol molecules thus the structure of the starch matrix becomes rigid.

3.7. *Thermomechanical analysis*

Dynamic mechanical testing of starch extrudates under programmed heating is considered as an appropriate method to determine the glass transition temperature (T_g) of these products provided a low frequency of oscillation (<1 Hz) is used. As it was previously mentioned most of the control samples were glassy, i.e. brittle and rigid whereas most of the extrudates containing fatty acids were flexible and their T_gs were lower than those exhibited by their control counterparts. Fig. 5 shows typical storage modulus (G') - temperature curves of the samples examined. It can be seen that the G' values of the control samples are higher than those of the samples contained myristic or palmitic acids. The results confirmed those obtained using the three-point bending test where it was shown that the control samples exhibited higher values of Young's modulus than their myristic acid containing counterparts. As for the glass transition temperature exhibited by the extrudates, Table 1 shows that the T_g values of the control samples were, in general, higher than those of the fatty acid containing extrudates indicating that glycerol participates in the starch matrix in a different fashion when an amylose complexing agent is present in the starch system.

3.8. *Scanning electron microscopy*

Extrusion processing is known to cause substantial changes in the physical characteristics of starch granules. It has been shown (Bhatnagar & Hanna, 1997; Raphaelides et al., 2010) that the granules completely disappear during extrusion even in the presence of fatty acids. However, in this work it was found that when starch was extruded in the presence of glycerol and fatty acids at 100 °C and at low screw speeds (20–91 rpm) a substantial part of starch granules remained intact albeit swollen at 20 rpm and a smaller number retained their shape at 91 rpm (Fig. 6a and b). On the contrary all control extrudates regardless of the barrel temperature and the screw speed employed showed (Fig. 6c) a continuous phase without any trace of starch granules. At screw speeds 161 and 227 rpm and at 100 °C barrel temperature no intact granules were found in fatty acid containing extrudates (Fig. 6d) and the same happened at higher temperatures. As it was previously mentioned, the presence of intact granules in the fatty acid containing samples should be attributed not so much to the lubricating effect of glycerol since the control samples also contained glycerol nevertheless they did

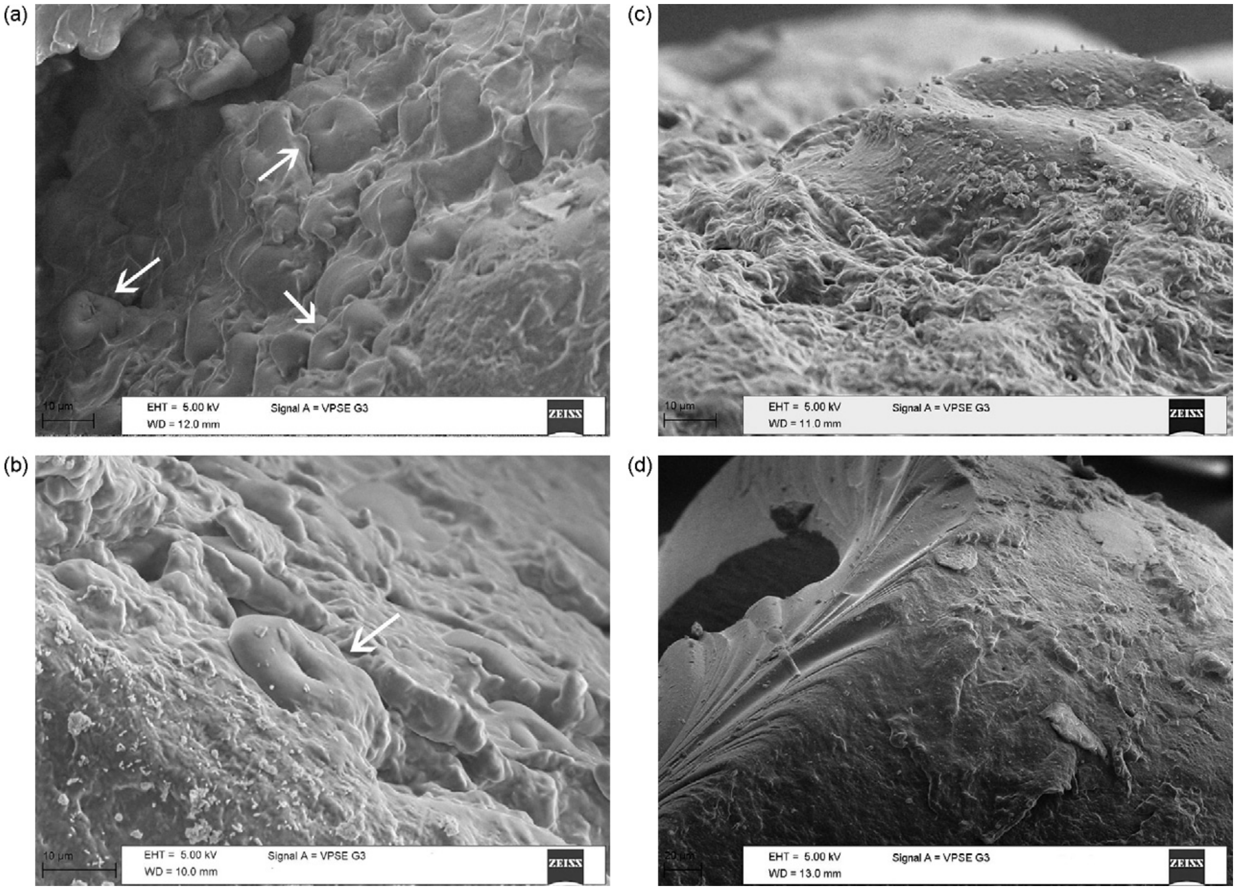

Fig. 6. SEM Micrographs of maize starch–glycerol extrudates with added fatty acids and without (control). (a) Myristic acid containing samples extruded at 100 °C and at 20 rpm screw speed. (b) Palmitic acid containing samples extruded at 100 °C and at 91 rpm. (c) Control sample extruded at 100 °C and at 91 rpm. (d) Myristic acid containing samples extruded at 100 °C and at 227 rpm.

not preserve intact granules in their matrix, but rather to the interaction of fatty acids with the amylose molecules located on the surface of the swollen granules which reinforced the granules to withstand the shearing forces developed during extrusion.

3.9. X-ray diffraction

Fig. 7 reveals the differences in X-ray diffraction patterns of maize starch extruded either with added glycerol or without glycerol or with added fatty acids and glycerol. It can be seen that the maize extrudate without glycerol shows a small amount of the typical V-type pattern crystallinity attributed to amylose complexation with the endogenous free fatty acids and lysophospholipids which are naturally present in native starch granules. When glycerol was added to starch the extrudate crystallites exhibited a mixture of V-type pattern and a presumably B-type pattern (peak at approximately 17° 2θ diffraction angle) attributed to amylose retrogradation on aging (van Soest & Knooren, 1997). On the other hand, extrudates containing both glycerol and fatty acids exhibited great amounts of the V-type crystallinity due to extensive amylose–fatty acid interactions. The results confirmed that glycerol's presence caused structural changes to starch matrix which were different in the fatty acid containing extrudates from the extrudates without fatty acids. Concerning the percentage crystallinity of the extrudates, Fig. 8 shows that there are no appreciable differences among the control samples and those which contained fatty acids and the same applies as far as the crystallite size is concerned (data not shown). The results indicate that since the crystallinity exhibited by the starch matrix is almost solely due to amylose, then all available amylose molecules of the extrudates were crystallized either because of retrogradation on aging, forming double helices (B-type crystallinity) or because of complexation with fatty acids, forming single helices (V-type crystallinity). Moreover, it has been reported (van Soest, Hulleman, de Wit, & Vliegenthart, 1996) that the formation of small amounts of B-type crystallinity increased the stiffness of extruded starch plasticized with glycerol, which explains the findings previously mentioned that the control samples appeared to be more rigid than the samples containing fatty acids.

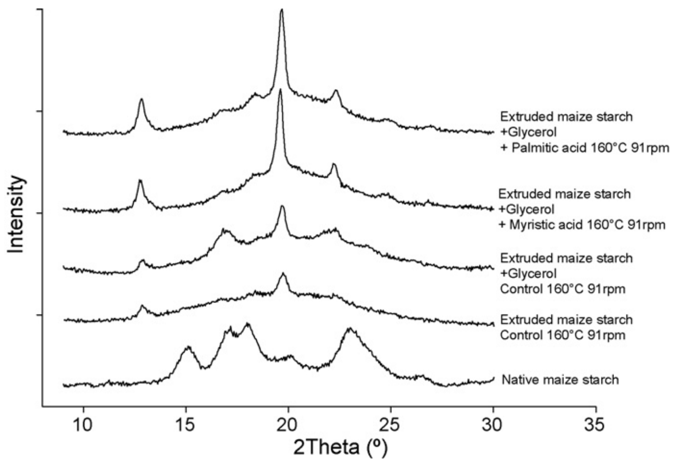

Fig. 7. X-ray diffraction patterns of maize starch either native or extruded with the addition of glycerol and fatty acids or with out at 160 °C barrel temperature and at 91 rpm screw speed.

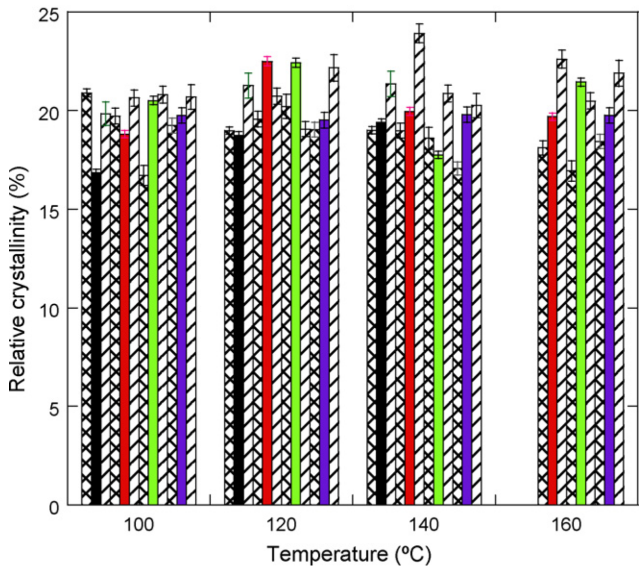

Fig. 8. Effect of screw speed and barrel temperature on the relative crystallinity of starch–fatty acid–glycerol extrudates. Symbols are the same as in Fig. 2.

4. Conclusions

The present work revealed that the combined effect of fatty acid and glycerol addition to maize starch systems during extrusion cooking caused significant changes in the structural characteristics of the extrudates which mainly influenced their mechanical properties. It was found that the role of glycerol as a plasticizer in starch extrudates was enhanced by the presence of fatty acid molecules in the starch matrix rendering the extrudates more flexible and less glassy than their counterparts which contained glycerol but no fatty acids. This behaviour was attributed to the interaction of the formed, during extrusion cooking, amylose–fatty acid complexes with glycerol molecules.

The results indicated that controlling the processing conditions during extrusion and adding fatty acids and glycerol to starch a series of products can be derived with tailor made functional properties suitable to be potentially utilized as biodegradable materials.

Acknowledgment

The financial support received from the European Union-Greek Ministry of Education through the "ARCHIMEDES" research program is gratefully acknowledged.

References

Anderson, R. A., Conway, H. F., Pfeifer, V. F., & Griffin, L. E. J. (1969). Gelatinization of corn grits by roll- and extrusion cooking. *Cereal Science Today*, *14*(4–7), 11–12.

Banks, W., & Greenwood, C. T. (1971). The conformation of amylose in dilute solution. *Stärke*, *23*, 300–314.

Bhatnagar, S., & Hanna, M. A. (1994). Extrusion processing conditions for amylose–lipid complexing. *Cereal Chemistry*, *71*, 587–593.

Bhatnagar, S., & Hanna, M. A. (1997). Modification of microstructure of starch extruded with selected lipids. *Starch/Stärke*, *49*, 12–20.

Biliaderis, C. G., & Seneviratne, H. D. (1990). On the supermolecular structure and metastability of glycerol monostearate-amylose complex. *Carbohydrate Polymers*, *13*, 185–206.

Bizot, H. (1983). Using the "G.A.B." model to construct sorption isotherms. In R. Jowitt, F. Escher, B. Hallström, H. F. T. Meffert, W. E. L. Spiess, & G. Vos (Eds.), *Physical properties of foods*. London: Applied Science Publishers, pp. 43–54.

Brundle, R. C., Evans, C. A., & Wilson, S. (1992). *Encyclopedia of materials characterization—Surfaces, interfaces, thin films*. Boston: Butterworth-Heinemann.

Carlson, T. L.-G., Larsson, K., Dinh-Nguyen, N., & Krog, N. (1979). A study of the amylose—Monoglyceride complex by Raman spectroscopy. *Stärke*, *31*, 222–224.

Colonna, P., Doublier, J. L., Melcion, J. P., de Monredon, F., & Mercier, C. (1984). Extrusion cooking and drum drying of wheat starch. I. Physical and macromolecular modifications. *Cereal Chemistry*, *61*, 538–543.

Colonna, P., & Mercier, C. (1983). Macromolecular modifications of manioc components by extrusion—Cooking with and without lipids. *Carbohydrate Polymers*, *3*, 87–108.

Cooke, D., & Gidley, M. J. (1992). Loss of crystalline and molecular order during starch gelatinisation: Origin of the enthalpic transition. *Carbohydrate Research*, *227*, 103–112.

Davidson, V. J., Paton, D., Diosady, L. L., & Larocque, G. (1984). Degradation of wheat starch in a single screw extruder: Characteristics of extruded starch polymers. *Journal of Food Science*, *49*, 453–458.

Della Valle, G., Kozlowski, A., Colonna, P., & Tayeb, J. (1989). Starch transformation estimated by the energy balance on a twin screw extruder. *Lebensmittel Wissenschaft und Technologie*, *22*, 279–286.

Godet, M. C., Tran, V., Delage, M. M., & Buleon, A. (1993). Molecular modelling of the specific interactions involved in the amylose complexation by fatty acids. *International Journal of Biological Macromolecules*, *15*, 11–16.

Greenwood, C. T. (1964). Viscosity-molecular weight relations. In R. L. Whistler (Ed.), *Methods in carbohydrate chemistry, vol. IV (Starch)*. USA: Academic Press, pp. 179–188.

Han, C. D. (1976). *Rheology in polymer processing*. USA: Academic Press., pp. 89–126.

Karkalas, J. (1985). An improved enzymic method for the determination of native and modified starch. *Journal of the Science of Food and Agriculture*, *36*, 1019–1027.

Karkalas, J., & Raphaelides, S. (1986). Quantitative aspects of amylose–lipid interactions. *Carbohydrate Research*, *157*, 215–234.

Launay, B., & Kone, T. (1984). Twin-screw extrusion cooking of corn starch: Flow properties of starch pastes. In P. Zeuthen, J. C. Cheftel, C. Eriksson, M. Jul, H. Leniger, P. Linko, G. Varela, & G. Vos (Eds.), *Thermal processing and quality of foods*. England: Elsevier Applied Science Publishers, pp. 54–61.

Lourdin, D., Bizot, H., & Colonna, P. (1997). «Antiplasticization» in starch–glycerol films? *Journal of Applied Polymer Science*, *63*, 1047–1053.

Mantzari, G., Raphaelides, S. N., & Exarhopoulos, S. (2010). Effect of sorbitol addition on the physicochemical characteristics of starch–fatty acid systems. *Carbohydrate Polymers*, *79*, 154–163.

Mercier, C., Charbonniere, R., Grebaut, J., & de la Gueriviere, J. F. (1980). Formation of amylose–lipid complexes by twin-screw extrusion cooking of manioc starch. *Cereal Chemistry*, *57*, 4–9.

Meuser, F., van Lengerich, B., & Stender, J. (1985a). Bildung von Stärkelipidkomlpexen durch Kochextrusion. 1 Teil: Herstellung und strukturelle Charakterisierung der Komplexe. *Getreide Mehl und Brot*, *39*, 205–211.

Meuser, F., van Lengerich, B., & Stender, J. (1985b). Bildung von Stärkelipidkomlpexen durch Kochextrusion. 2 Teil: Funktionelle Eigenschaften der Extrudate. *Getreide Mehl und Brot*, *39*, 309–314.

Morrison, W. R., & Laignelet, B. (1983). An improved colorimetric procedure for determining apparent and total amylose in cereal and other starches. *Journal of Cereal Science*, *1*, 9–20.

Parker, R., Ollett, A.-L., & Smith, A. C. (1990). Starch melt rheology: Measurement, modeling and applications to extrusion processing. In P. Zeuthen (Ed.), *Processing and quality of foods, vol. 1* (pp. 1290–1295). England: Elsevier Applied Science Publishers.

Parker, R., & Ring, S. G. (2001). Aspects of the physical chemistry of starch. *Journal of Cereal Science*, *34*, 1–17.

Raphaelides, S. N. (1992). Flow behaviour of starch–fatty acid systems in solution. *Lebensmittel Wissenschaft undTechnologie*, *25*, 95–101.

Raphaelides, S. N., Arsenoudi, K., Exarhopoulos, S., & Xu, Z.-M. (2010). Effect of processing history on the functional and structural characteristics of starch–fatty acid extrudates. *Food Research International*, *43*, 329–341.

Snape, C. E., Morrison, W. R., Maroto-Valer, M. M., Karkalas, J., & Pethrick, R. A. (1998). Solid state ^{13}C NMR investigation of lipid ligands in V-amylose inclusion complexes. *Carbohydrate Polymers*, *36*, 225–237.

Steffe, J. F. (1996). *Rheological methods in food process engineering* (2nd ed.). USA: Freeman Press., p. 10.

Stäger, G. Über die Interaktionen von Emulgatoren mit Stärke bei der Heissextrusion, Doctoral Dissertation. Zürich:Eidgenössischen Technischen Hochschule Zürich (1988).

Stribeck, N. (2007). *X-ray scattering of soft matter*. Berlin: Springer.

van Lengerich, B. (1989). Influence of extrusion processing on in-line rheological behavior, structure and function of wheat starch. In H. Faridi, & J. M. Faubion (Eds.), *Dough rheology and baked product texture*. New York: Avi Publishing, pp. 421–471.

van Soest, J. J., Hulleman, S. H. D., de Wit, D., & Vliegenthart, J. F. G. (1996). Changes in the mechanical properties of thermoplastic potato starch in relation with changes in B-type crystallinity. *Carbohydrate Polymers*, *29*, 225–232.

van Soest, J. J., & Knooren, N. (1997). Influence of glycerol and water content on the structure and properties of extruded starch plastic sheets during aging. *Journal of Applied Polymer Science*, *64*, 1411–1422.